Water Research 215 (2022) 118208

Contents lists available at ScienceDirect

Water Research

journal homepage: www.elsevier.com/locate/watres

# Pilot scale microbial fuel cells using air cathodes for producing electricity while treating wastewater

Ruggero Rossi [a], Andy Y. Hur [b], Martin A. Page [b,**], Amalia O'Brien Thomas [c], Joseph J. Butkiewicz [c], David W. Jones [a], Gahyun Baek [a], Pascal E. Saikaly [d,e], Donald M. Cropek [b], Bruce E. Logan [a,*]

[a] Department of Civil and Environmental Engineering, The Pennsylvania State University, University Park, PA 16802, USA
[b] U.S. Army Corps of Engineers, Engineer Research and Development Center, Construction Engineering Research Laboratory, Champaign, IL 61822, USA
[c] Tobyhanna Army Depot, Tobyhanna, PA 18466, USA
[d] Environmental Science and Engineering Program, Biological and Environmental Science and Engineering Division, King Abdullah University of Science and Technology (KAUST), Thuwal 23955-6900, Kingdom of Saudi Arabia
[e] Water Desalination and Reuse Center, King Abdullah University of Science and Technology, Kingdom of Saudi Arabia

ARTICLE INFO

*Keywords:*
Microbial fuel cell (MFC)
Biofiltration (BF)
Wastewater
Energy from waste

ABSTRACT

Microbial fuel cells (MFCs) can generate electrical energy from the oxidation of the organic matter, but they must be demonstrated at large scales, treat real wastewaters, and show the required performance needed at a site to provide a path forward for this technology. Previous pilot-scale studies of MFC technology have relied on systems with aerated catholytes, which limited energy recovery due to the energy consumed by pumping air into the catholyte. In the present study, we developed, deployed, and tested an 850 L (1400 L total liquid volume) air-cathode MFC treating domestic-type wastewater at a centralized wastewater treatment facility. The wastewater was processed over a hydraulic retention time (HRT) of 12 h through a sequence of 17 brush anode modules (11 $m^2$ total projected anode area) and 16 cathode modules, each constructed using two air-cathodes (0.6 $m^2$ each, total cathode area of 20 $m^2$) with the air side facing each other to allow passive air flow. The MFC effluent was further treated in a biofilter (BF) to decrease the organic matter content. The field test was conducted for over six months to fully characterize the electrochemical and wastewater treatment performance. Wastewater quality as well as electrical energy production were routinely monitored. The power produced over six months by the MFC averaged 0.46 ± 0.35 W (0.043 W $m^{-2}$ normalized to the cross-sectional area of an anode) at a current of 1.54 ± 0.90 A with a coulombic efficiency of 9%. Approximately 49 ± 15 % of the chemical oxygen demand (COD) was removed in the MFC alone as well as a large amount of the biochemical oxygen demand ($BOD_5$) (70%) and total suspended solid (TSS) (48%). In the combined MFC/BF process, up to 91 ± 6 % of the COD and 91 % of the $BOD_5$ were removed as well as certain bacteria (*E. coli*, 98.9%; fecal coliforms, 99.1%). The average effluent concentration of nitrate was 1.6 ± 2.4 mg $L^{-1}$, nitrite was 0.17 ± 0.24 mg $L^{-1}$ and ammonia was 0.4 ± 1.0 mg $L^{-1}$. The pilot scale reactor presented here is the largest air-cathode MFC ever tested, generating electrical power while treating wastewater.

## 1. Introduction

Around 600 billion kWh of energy are contained in the organic matter of the 300 billion $m^3$ per year of domestic wastewater generated worldwide (Lu et al., 2018) considering an average energy content of 2 kWh $m^{-3}$ (Heidrich et al., 2011), making the recovery of the energy contained in these waste streams a compelling opportunity to achieve a circular economy and diminish the high energy cost of wastewater treatment. Microbial fuel cells (MFCs) can potentially reduce energy consumption for wastewater treatment by generating electricity while oxidizing organic matter in the wastewater (Do et al., 2018; Munoz-Cupa et al., 2021). In an MFC, oxidation of the biodegradable organic

* Corresponding author.
** Co-corresponding author.
*E-mail addresses:* martin.a.page@usace.army.mil (M.A. Page), blogan@psu.edu (B.E. Logan).

https://doi.org/10.1016/j.watres.2022.118208
Received 13 September 2021; Received in revised form 23 October 2021; Accepted 15 February 2022
Available online 17 February 2022

matter by exoelectrogenic bacteria on the anode is coupled with the oxygen reduction reaction (ORR) at the cathode to produce electrical power (Logan et al., 2019). MFCs have primarily being tested in lab- or bench-scale reactors, often using only synthetic wastewaters characterized by high buffer capacities and substrate concentrations that are not representative of typical domestic wastewaters (Logan et al., 2015). MFCs need to be demonstrated at pilot-scale, treating real waste streams, and showing sufficient performance to provide a path forward for implementation of this technology (Zhang et al., 2013).

Scaling up MFCs is technically challenging due to the need for a high electrode packing density ($m^2$ of electrode per $m^3$ of reactor) while increasing reactor capacity to maximize the reactor performance. If the electrode specific surface area is not maintained during reactor scale up from lab- to pilot scale, the volumetric power densities will decrease due to the lack of sufficient electrode specific surface area (Logan et al., 2015). MFCs with low electrode packing densities typically produce low volumetric power due to the large spacing between the electrodes, which increases the solution resistance and restricts the performance of the reactor (Rossi et al., 2020). However, maintaining a similar electrode packing density during scale-up requires cathodes able to withstand high water head pressure in order to avoid flooding of the cathode and the cathode chamber (Dekker et al., 2009). The ORR at the cathode uses oxygen to consume electrons generated by the anode. Thus, the ORR catalyst needs to be in contact with either dissolved oxygen in liquid media or with air (Popat and Torres, 2016; Rossi et al., 2020). Most of the previous MFC pilot scale reactors larger than 250 L have used wastewater aeration rather than direct air cathodes (Feng et al., 2014; Liang et al., 2018, 2019; Vilajeliu-Pons et al., 2017). Wastewater aeration is undesirable as it currently consumes about half the energy used at a treatment plant, and therefore direct air cathodes are preferred to reduce energy demands. However, as the volume of the reactor and the electrode dimensions are increased, the water pressure on the liquid side of the cathode can result in leakage and water flooding of the cathode chamber. One of the largest air-cathode reactors constructed to date (250 L) had horizontal plug flow across two cathodes each 1 $m^2$, separated by 25 cm, in order to minimize hydrostatic pressure and prevent water leakage (Feng et al., 2014). The MFC module produced a power density of 0.057 ± 0.001 W $m^{-2}$ with a COD removal rate of 76.3%. The MFC was estimated to reduce energy costs compared to a conventional wastewater treatment by half, although expensive precious metal catalysts increased the capital costs of the reactor. The Pt/C cathodes accounted for up to 50% of the overall cost of the MFC. A new cathode with no precious metal catalyst and capable of withstanding higher water heights (0.7 m) was recently developed (Hiegemann et al., 2019; Rossi et al., 2019a, 2019b). The window-pane architecture of these cathodes contained panels using activated carbon catalysts, with the cathodes welded and glued into a stainless-steel frame. The cathode was used in MFCs to produce a maximum power density of 0.101 ± 0.006 W $m^{-2}$ with 0.62 $m^2$ of cathode in a reactor of 85 L (7.3 $m^2$ $m^{-3}$) which was of the same order of magnitude of the power densities obtained in smaller, laboratory scale MFCs fed domestic wastewater (0.31 ± 0.01 W $m^{-2}$ in a reactor of 28 mL) (Rossi et al., 2019).

In this study, we developed and tested the largest air-cathode MFC using primarily domestic wastewater generated at a field site (Tobyhanna Army Depot, US). Multi-panel cathodes (32) each containing 15 activated carbon cathode panels (0.032 $m^2$ each, total active area = 15 $m^2$) were welded into metal sheets, producing a total cathode surface area of 20 $m^2$. These cathodes were placed into 0.85 $m^3$ of the tank that had a total volume of 1.4 $m^3$ (volume including influent and effluent zones) achieving a final electrode packing density of 23 $m^2$ $m^{-3}$. This packing density was comparable to that obtained in much smaller MFCs (25 $m^2$ $m^{-3}$) (Logan et al., 2015), therefore achieving negligible loss (< 6%) in electrode packing densities with increased reactor size. The MFC was integrated into an existing wastewater treatment facility at the site, and the effluent of the MFC provided the influent to a biofiltration (BF) unit (Ward et al., 2015) to further treat the wastewater to meet low effluent COD requirements. The combined MFC and BF technologies were designed, assembled, and integrated into an automated pilot scale wastewater treatment skid that could treat up to 3.79 liters-per-minute (Lpm) of wastewater. The combined treatment system was assessed over a six-month period, from September 2020 through April 2021, despite having limited personnel at the site due to the COVID 19 pandemic. Over the course of the pilot study, the system performance was measured in terms of water quality and energy production and consumption for various relevant modes of operation.

## 2. Materials and methods

### 2.1. Construction and operation of the MFC

The MFC (Intuitech, Utah) was a 1400 L (including inlet and outlet, 850 L active electrolyte occupied by anode and cathode modules) PVC tank, 2.4 m long by 1.2 m wide by 0.7 m tall (Fig. 1). The wastewater was fed through a manifold to distribute the flow across the height of the module and the wastewater effluent from the MFC was delivered by gravity to the BF unit. The MFC contained 17 anode modules (Supporting Information) with 40 carbon fiber brush anodes each, made using two twisted titanium wires (2.5 cm diameter, 61 cm brush length, 71 cm overall length). The total anode projected area was 11 $m^2$. The brush anodes of each module were electrically connected and wired to the control panel. Cathodes (1.1 m wide by 0.6 m long, 0.62 $m^2$ exposed area, 0.48 $m^2$ electroactive area due to the stainless-steel frame) were purchased from VITO (Belgium, Mol) following a design previously described (Rossi et al., 2019b) and assembled in the final cathode module. The cathodes were manufactured to be permeable to air on one side (30% diffusion layer porosity) and impermeable to water on the other side, using a proprietary manufacturing process (Bouwman et al., 2020). Each cathode module (16 total – 2 cathodes each) (Supporting Information) was assembled using two air cathodes secured 5 cm apart in the module with the air sides facing each other (air chamber) and the solution side in contact with the wastewater in the MFC. To reduce the cathode deformation due to the pressure of the water on the cathode, a support structure that was integral to the side plates of the cathodes was used in the air chamber (Supporting Information). The electrode spacing between anode and cathode was 1.2 cm. The anode modules closer to the MFC influent and effluent were connected to one cathode each. The remaining anode modules (15) were connected to two cathodes, one on each side of the brushes. The cathodes were wired to the control board and the anode-cathode voltage and current were continuously recorded with a multimeter (Keithley 2700 and 2750). The control board performed maximum power point tracking and allowed continuous measurement of each anode-cathode pair performance in terms of current and voltage produced, avoided voltage reversal, and boosted the final voltage output to either 12 V, 18 V or 24 V. The design of the pilot scale MFC is described in greater detail in the Supporting Information.

The performance of the MFC was continuously evaluated through measurement of the current, voltage, and power output from each anode-cathode pair (32 channels). The power and current density were normalized by the cross-sectional area of the anode module (0.62 $m^2$ each, 11 $m^2$ total) or the cathode module (0.62 $m^2$ each, 20 $m^2$ total). The volumetric power was normalized by the active volume of the MFC (850 L), neglecting the inlet and outlet zones as these areas were included to facilitate sampling, inspection, and troubleshooting. During the initial three months of operation, voltage and current were monitored with a separate multimeter (Keithley 2700 voltmeter) by connecting each anode module to the two cathodes closest to it through a 4.9 ± 0.6 Ω external resistor. Following the startup and acclimation phase in the initial three months of operation, the control board was installed in the control panel allowing a continuous monitoring of the current, voltage and power output of the MFC. The MFC net energy recovery (NET) was calculated by normalizing the kWh produced over

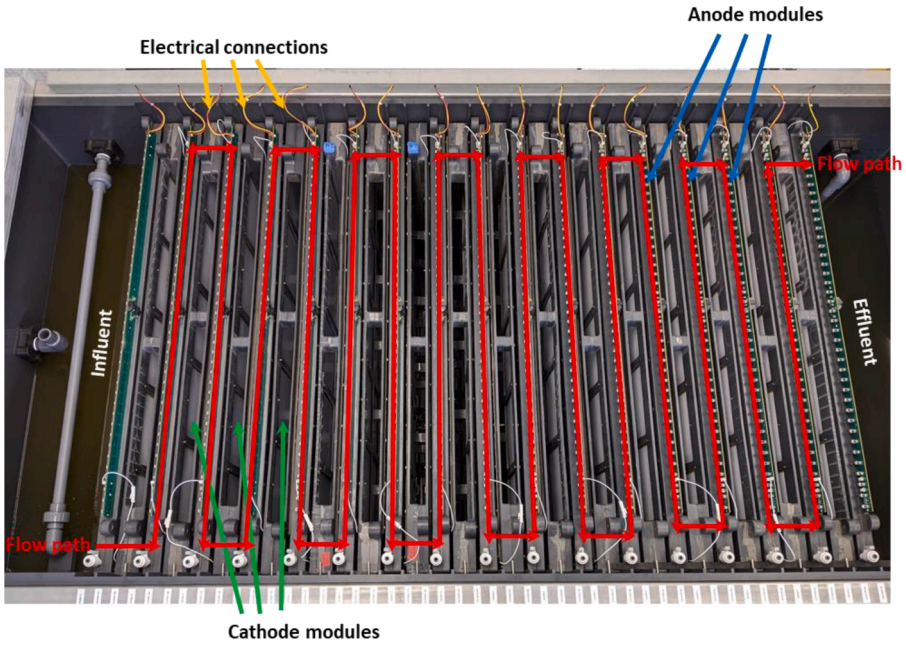


**Fig. 1.** Top view of the pilot MFC showing the electrical connections (yellow arrows) anode (blue arrows) and cathode modules (green arrows) and the wastewater flow path (red arrows).

six months by the amount of wastewater treated (Wh $m^{-3}$) or COD degraded (Wh $kg_{COD}^{-1}$). Sampling methods and additional details on the inoculation and operation of the pilot scale MFC-BF are described in greater detail in the Supporting Information.

### 2.2. Effluent treatment using the BF

After wastewater treatment in the MFC, a BF polishing system (Fig. 2) was utilized to provide further reduction of COD and suspended solids. The BF system employs high surface area granular activated carbon filtration media that is biologically active, allowing for simultaneous physical and biological treatment via adsorption and subsequent biodegradation of both dissolved and particulate contaminants. The pilot scale BF unit was composed of a 76 L PVC rectangular tank for feed water, two upflow 300 L Plexiglass hexagonal tanks (0.33 $m^2$ area by 0.9 m tall) filled two thirds of the height with 200 L activated carbon (AquaCarb 816, Evoqua, USA), and a 76 L PVC rectangular water holding tank for ultrafiltration (UF) feed, followed by a UF module (Cantel FiberFlo hollow fiber cartridge, 0.2 micron filter size, 7.4 cm outside diameter, 51 cm length) and a UV device for disinfection (Aquisense Technologies, Erlanger, Kentucky, USA). The BF unit was continuously fed by a suction pump to maintain a design flux of 5.76 Lpm/$m^2$ while loading. The air operated pinch valves were integrated to control the flow path during BF loading and bioregeneration phases.

**Fig. 2.** Photo of the BF skid.

## 3. Results and Discussion

### 3.1. MFC performance

The total power produced by the MFC quickly increased during the inoculation stage from 0.01 W to 0.65 W (1.5 A) over the initial three days of operation, producing an average power density for each module of 0.061 ± 0.008 W $m^{-2}$ (normalized by anode area, 11 $m^2$), indicating that the MFC was capable of delivering power in less than a week following inoculation. The average power produced over six months was 0.46 ± 0.35 W (0.54 ± 0.41 W $m^{-3}$) at an average current of 1.54 ± 0.90 A. The average power density of the pilot MFC was 0.023 ± 0.017 W $m^{-2}$ (0.077 ± 0.045 A $m^{-2}$) normalized by cathode surface area (20 $m^2$) and 0.043 ± 0.033 W $m^{-2}$ (0.145 ± 0.085 A $m^{-2}$) normalized by the anode surface area (11 $m^2$). The MFC maximum power was 1.43 W (1.68 W $m^{-3}$) at 2.95 A, recorded 81 days after inoculation.

At the maximum power point, the power density was 0.135 W $m^{-2}$ at a current density of 0.278 A $m^{-2}$ based on the anode surface area (or 0.072 W $m^{-2}$ normalized by cathode area). This maximum power density was 34% higher than that obtained with an 85 L MFC (0.101 ± 0.006 W $m^{-2}$) that used similar materials based on polarization data (Rossi et al., 2019a). Here two cathodes were connected to one anode compared to only one cathode per anode in the previous study. Doubling the cathode surface area has been shown to increase power, although not directly in proportion to the cathode area. For example, doubling the cathode area

increased the maximum power by 62% in a 0.028 L reactor (Cheng and Logan, 2011), 39-53% in a 0.1 L MFC (Kim et al., 2015) and by 67% in a 6.1 L MFC (He et al., 2016). A polarization curve was obtained after 81 days of operation from three modules in the MFC by decreasing the external resistance from 100 Ω to 0.5 Ω allowing 20 minutes between one resistance and the next to allow the voltage to stabilize. The maximum power density was 0.172 ± 0.003 W $m^{-2}$, with an internal resistance of 1.00 ± 0.04 Ω $m^2$ determined from the slope of the polarization curve near the maximum power point (Supporting information, Figure S10). The large difference in performance between continuous operation (0.135 W $m^{-2}$) and the polarization curve (0.172 ± 0.003 W $m^{-2}$) indicates that the power density was overestimated during the polarization test due to the rapid change in resistances over time (20 minutes), which has been proved to be effective in small scale systems, but which does not allow large electrodes to fully discharge their capacitive current (Liang et al., 2019; Velasquez-Orta et al., 2009).

After the initial inoculation stage with fed-batch operation, wastewater was fed to the MFC at different flow rates, producing changes in MFC performance primarily due to variations in the organic content of the wastewater and the rate of wastewater flow into the system (Fig. 3). The low population on the site during nights, weekends, and holidays did not allow for a stable and continuous feed of wastewater in the MFC, which was further complicated by the reduced personnel on site due to COVID 19 occupancy restrictions. The wastewater flow rate was changed from 1.89 Lpm during the day (8 am – 3 pm), five days a week, to 0.76 Lpm overnight (3 pm – 8 am), and completely interrupted (0 Lpm) during the weekends. The lower flow rate overnight decreased the organic loading fed to the MFC, diminishing the total power produced by the MFC (Fig. 3). After 80 days of operation, the maximum power peaked at 1.30 W at 8 pm, decreasing by 35% to 0.84 W at 11 am the following day due to the lower flowrate overnight. The lag time between the decrease of the flow rate and the decrease in the performance was likely due to the high HRT of the MFC (12 h at 1.89 Lpm and 30 h with 0.76 Lpm). Interrupting the wastewater flow during the weekend further decreased the total power to only 0.03 W before restarting the system the following week. The large impact of the flow rate on the performance indicated that the MFC performance was primarily limited by the low organic loading during the weekends at low flow rates, and that the MFC power generation can be increased by maintaining a high COD content in the system. Even though the power decrease at low flow rates was substantial, the MFC performance quickly recovered as soon as the wastewater feed was reestablished, indicating a high resiliency of the reactor to operational shocks such as low COD concentrations (Fig. 3).

The anode-cathode pairs produced variable current and power depending on their position in the MFC (Fig. 4). The modules closer to the inlet and outlet produced an average of 46% less power than the modules positioned in the middle of the tank, likely due to the larger intrusion of air into the media and to the lower cathode surface area. Only one cathode was connected to the anode modules next to the

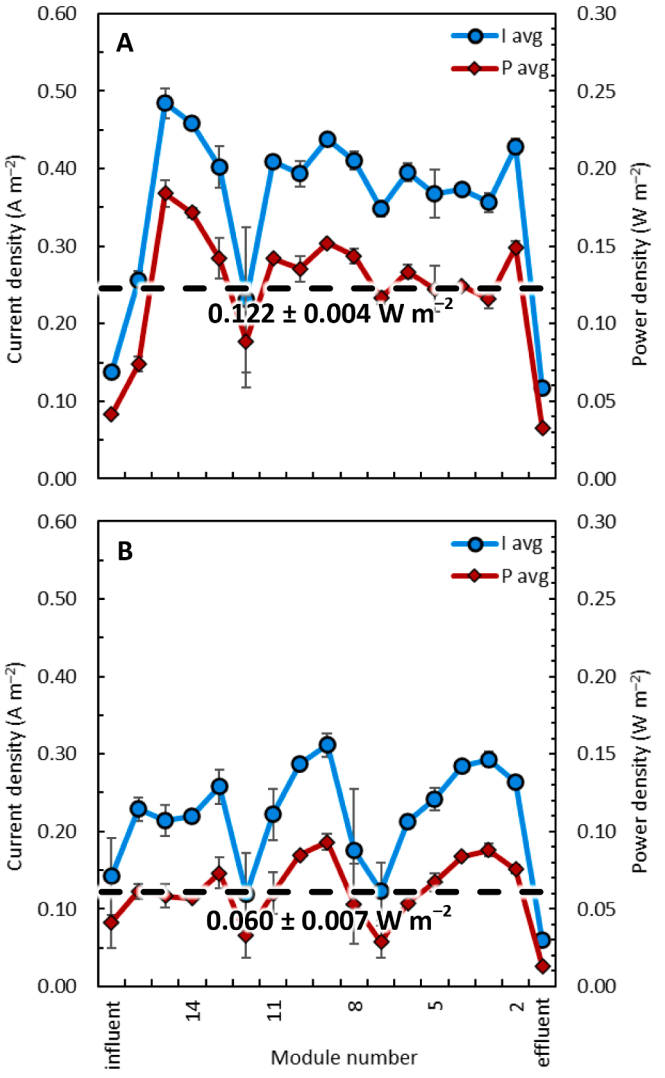


**Fig. 4.** Performance of the different electrode modules throughout the MFC after (A) 3 months and (B) 6 months of operation. Current density and power density of each module (17) normalized by the anode cross sectional area (0.62 $m^2$ – one anode connected with two cathodes).

influent and effluent manifolds while two cathodes each were used for the remaining anode modules (Fig. 1). After three months of operation, the average power density over 9 hours of operation of the module next to the inlet was 0.041 ± 0.001 W $m^{-2}$, similar to the last module just before the wastewater outlet (0.033 ± 0.002 W $m^{-2}$). This power density

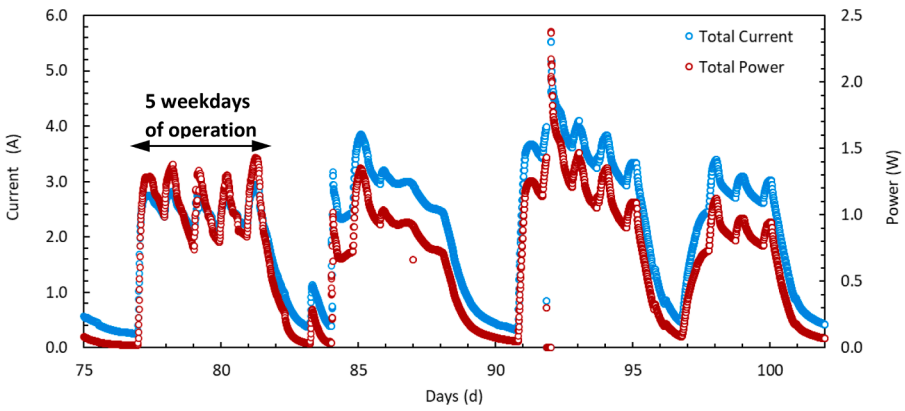


**Fig. 3.** Total power and current produced by the MFC over four weeks of continuous operation. The average current and power density and the total current and power produced over the whole test duration are reported in the Supporting Information. The large power and current (2.38 W at 5.53 A) produced at day 92 was due to the discharge of the charges accumulated during maintenance of the MFC and the control board. Once the board was reconnected, the charge accumulated in the electrodes was immediately discharged resulting in a large power and current production, which could not be maintained over time.

was 73% smaller than that produced by the module in the middle of the MFC (0.152 ± 0.003 W $m^{-2}$). Normalizing the power by the cathode surface area slightly decreases the difference in performance between the end modules and the other modules in the middle of the MFC (average 0.077 ± 0.003 W $m^{-2}$), suggesting that oxygen intrusion can be a factor in limiting the performance of the anodes.

The average power density of the MFC decreased by 60% after six months of operation, from 0.122 ± 0.003 W $m^{-2}$ (total power of 1.3 W) to 0.060 ± 0.007 W $m^{-2}$ (total power of 0.6 W). Part of this decrease was due to cathode fouling. For example, the performance of an 85 L MFC using a cathode having a design similar to the one used here decreased by 28% after one month of operation, primarily due to inorganic and biofouling of the cathode over time (Rossi et al., 2019b). Some of this degradation in performance over time is due to the formation of a biofilm on the cathode, the deposition of salts in the electrocatalytic structure, and the adsorption of the organic matter present in the wastewater onto the cathode (An et al., 2017). In addition, the decrease in the average power density for the total reactor was due to failure of water integrity of five cathode modules. These modules developed leaks which resulted in flooding of the air chambers, producing a large decrease in the performance of those anode-cathode modules. When the cathode chamber becomes filled with water there is little or no dissolved oxygen in the water, and thus current generation is inhibited unless the water is sparged with air (Vilajeliu-Pons et al., 2017).

### 3.2. Microbial community analysis

The microbial community on the anode and cathode electrodes was analyzed after eight months of operation (Fig. 5). *Sulfurimonas* and *Desulfobacter* were the most abundant genera on the electrodes of the MFC. While the relative abundance of *Sulfurimonas* increased from the influent to the outlet of the reactor, *Desulfobacter* followed the opposite trend, being most present on the electrodes closer to the influent compared to the effluent. *Desulfobacter* is a sulfate-reducing bacterium

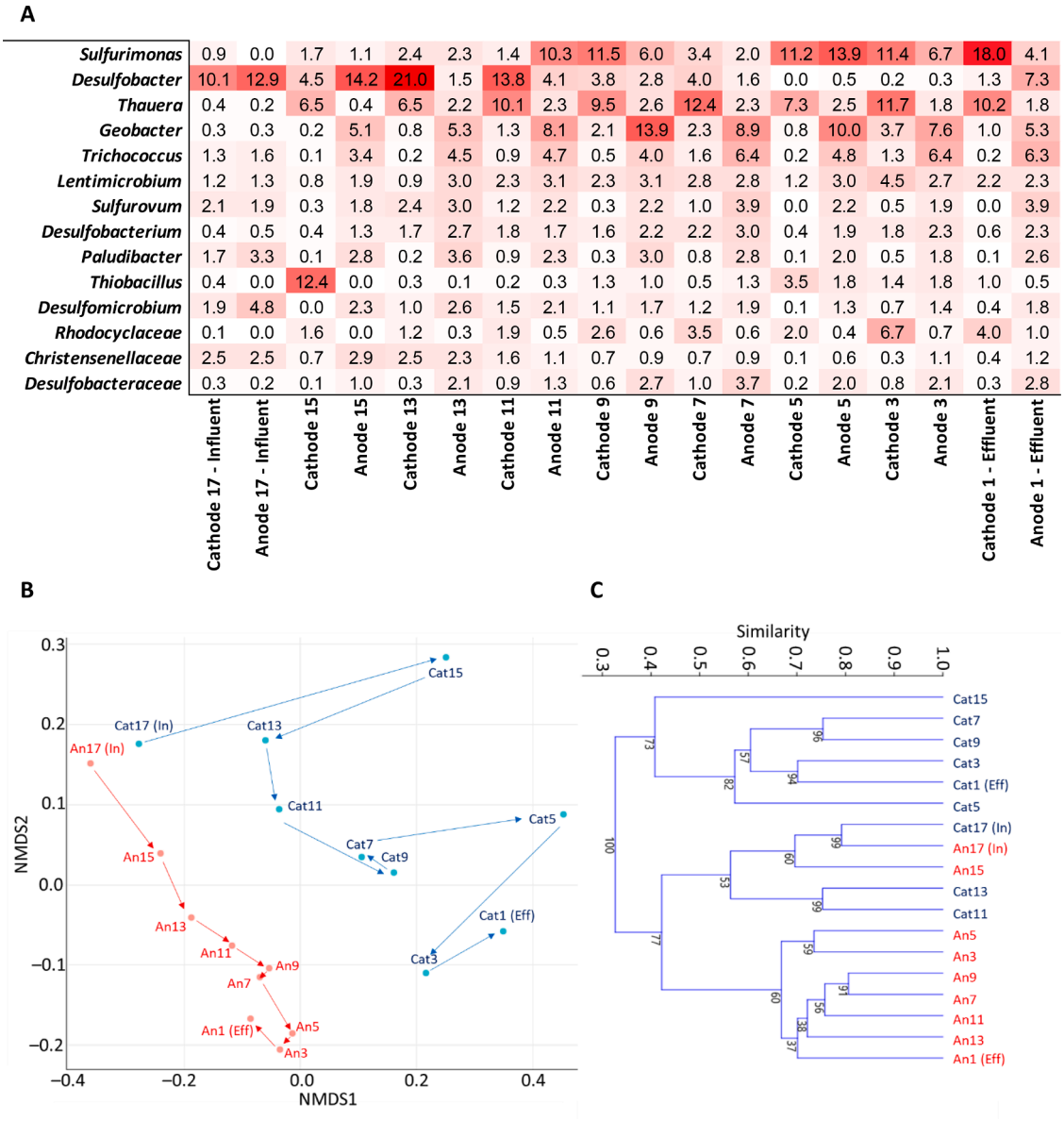


**Fig. 5.** (A) Heatmap of the 14 most abundant genera throughout the MFC modules, from the MFC influent (17) to the MFC outlet (1). Only one cathode of the two connected to the anode was sampled. Values are shown as normalized fraction of total sequences (%). (B) Nonmetric multidimensional scaling plots and (C) cluster dendrograms constructed based on the 200 most abundant OTUs. Microbial community profiles are labeled with the corresponding biomass collection location (An, anode; Cat, cathode; In, influent; Eff, effluent).

and was likely involved in the reduction of sulfate to sulfide as the wastewater flows through the MFC. Then, due to the presence of the air cathodes and residual dissolved oxygen in solution, *Sulfurimonas* took over, oxidizing the sulfide produced by *Desulfobacter*. This synergistic activity can be observed from the network analysis results, indicating a significant ($p$-value $< 0.05$) negative correlation between the two operational taxonomic units (OTUs) (Supporting Information). *Geobacter, Trichococcus, Desulfobacterium, Paludibacter* and *Thauera* showed an unequal distribution between anodes and cathodes. *Geobacter* and *Trichococcus* were primarily concentrated on the anode. *Trichococcus* have rarely been reported on MFC anodes, and typically only when solutions with high concentration of ammonia are fed to the reactor (Liu et al., 2019). *Geobacter* is a well-known exoelectrogenic bacteria (Holmes et al., 2004), and its distribution in the pilot MFC followed the same trend of the power density of the different modules (Fig. 4), showing the highest concentration of *Geobacter* in the modules in the middle of the MFC, and the lowest in the anode modules closer to the influent and effluent. The MFC modules next to the inlet and outlet were open to air, in order to facilitate troubleshooting of the MFC and sampling. However, it has been previously shown that *Geobacter* can tolerate and even utilize small amounts of oxygen to sustain its metabolism (Lin et al., 2004). High dissolved oxygen concentrations, however, are detrimental to the bacterium, suggesting that the oxygen intrusion in the wastewater close to the MFC influent and effluent could have limited its activity and the development of an exoelectrogenic biofilm. *Desulfobacterium* and *Paludibacter* have been previously identified on MFC anodes in several studies (Huang et al., 2012; Kim et al., 2011; Li et al., 2021; Liang et al., 2013; Wang et al., 2019). *Thauera*, which selectively colonized the cathode, was previously detected in MFC studies, more predominantly on the cathode (Shehab et al., 2013; Yang et al., 2019, 2018; Zhang et al., 2015). Members of the genus *Thauera* are known to play a role in denitrification (Daims et al., 2010) and they were previously detected in MFCs operated for nitrogen removal (Sayess et al., 2013). The detection of known genera responsible for nitrification such as *Nitrosomonas, Nitrobacter*, and *Nitrospira* (Sayess et al., 2013) at low relative abundance (0.13-0.16%), coupled with the presence of nitrate and nitrite (Section 3.3) in the MFC reactor, and the presence of *Thauera*, suggest the possibility of nitrification and denitrification occurring in the MFC reactor. The overall microbial community structures collected from anodes and cathodes grew apart with the flow of wastewater (i.e., from inlet to outlet) (Fig. 6). The community of anode17 and cathode17, which were located closest to the wastewater inlet, had high similarity but diverged greatly with the wastewater flowing to the outlet. From the middle to the outlet, the electrochemical environment strongly influenced the divergence of microbial communities which were clustered by anode or cathode.

### 3.3. MFC/BF wastewater treatment performance

A total volume of 110 $m^3$ of wastewater was treated during the six-month period of operation of the MFC, with an average COD removal of 49 ± 15 % in the MFC alone, and an overall 91 ± 6 % COD removal for the combined MFC/BF technology (Fig. 6A). The average COD in the MFC influent was 425 ± 114 mg $L^{-1}$ which was decreased to 220 ± 105 mg $L^{-1}$ in the MFC effluent, and to 36 ± 23 mg $L^{-1}$ in the BF effluent. Using the average COD removal in the MFC and the average current produced by the MFC resulted in a Coulombic efficiency of approximately 9%. The BF effluent was a clear liquid with no appreciable content of dispersed solids (Supporting Information). The TSS concentration was reduced by 48 ± 17 % in the MFC, from an average of 123 ± 23 mg $L^{-1}$ to 61 ± 17 mg $L^{-1}$ (Fig. 6B). The turbidity of the media decreased by 78% in the MFC and by an overall 97% post BF treatment (Supporting Information), in line with the decrease of COD and TSS. The average MFC influent turbidity was 60 NTU, while the MFC effluent was 12 NTU and the BF effluent was 1 NTU, indicating that most of the solids and particulate dispersed in solution was effectively removed during the MFC/BF treatment.

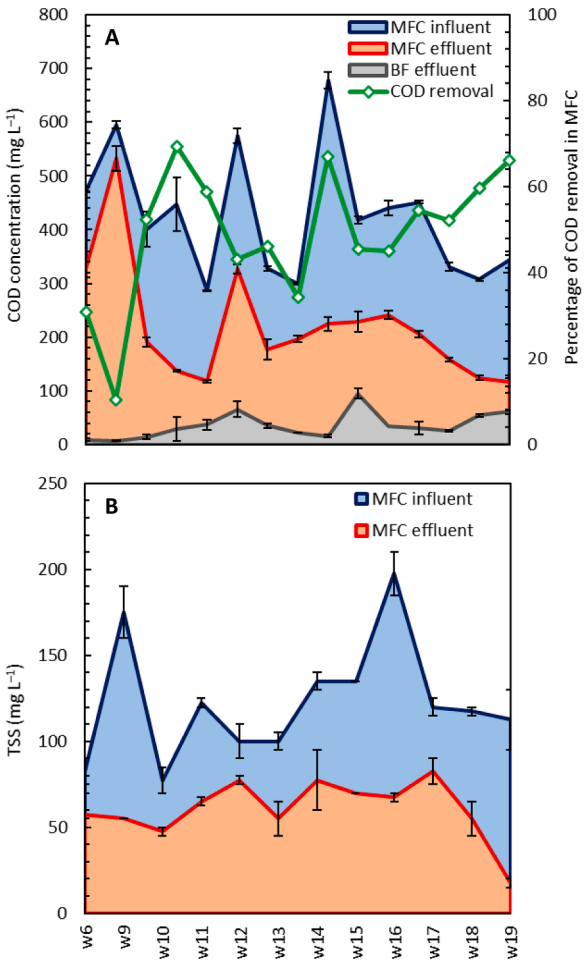


**Fig. 6.** (A) COD consumption and (B) TSS concentration in the MFC and BF over time (week 6 to 19).

The concentration of ammonia, nitrite, and nitrate in the MFC influent, MFC effluent and post BF treatment was monitored after the inoculation stage of the MFC and throughout the whole study (Fig. 7). The average ammonia concentration detected in the MFC influent was 33 ± 27 mg $L^{-1}$ and decreased by around 92% to 2.5 ± 2 mg $L^{-1}$ in the MFC effluent. The ammonia concentration in the BF effluent averaged 0.4 ± 1 mg $L^{-1}$. Previous studies have reported an ammonia removal in MFCs of approximately 60% for single-chamber, air cathode MFCs (Jung et al., 2008). The ammonia is typically removed in MFCs by volatilization due to the conversion of ammonium ion to the more volatile ammonia species because of an elevated pH near the cathode (Jung et al., 2008; Motoyama et al., 2021). However, we cannot exclude the possibility of nitrification and denitrification occurring in the MFC reactor due to the presence of nitrate and nitrite and known genera responsible for nitrification and denitrification (Liang et al., 2021; Motoyama et al., 2021; Yuan et al., 2021; Zheng et al., 2020).

Nitrite concentrations decreased after treatment by the MFC from 0.16 ± 0.04 mg $L^{-1}$ to 0.06 ± 0.02 mg $L^{-1}$. The average concentration of nitrite in the BF effluent from week 6 to week 13 from startup was 0.03 ± 0.04 mg $L^{-1}$ and then increased in last few weeks of operation to 0.32 ± 0.27 mg $L^{-1}$ (week 13-19) (Supporting Information). The increase in the nitrite concentration in the BF effluent was likely due to nitrification due to the higher loading of wastewater treated by the BF unit in the last weeks of the demonstration. The BF was initially bypassed due to frequent clogging of the ultrafiltration unit and overflow in one granular activated carbon tank. Once these issues were resolved, the BF was operated on a daily basis treating the MFC effluent. The nitrate

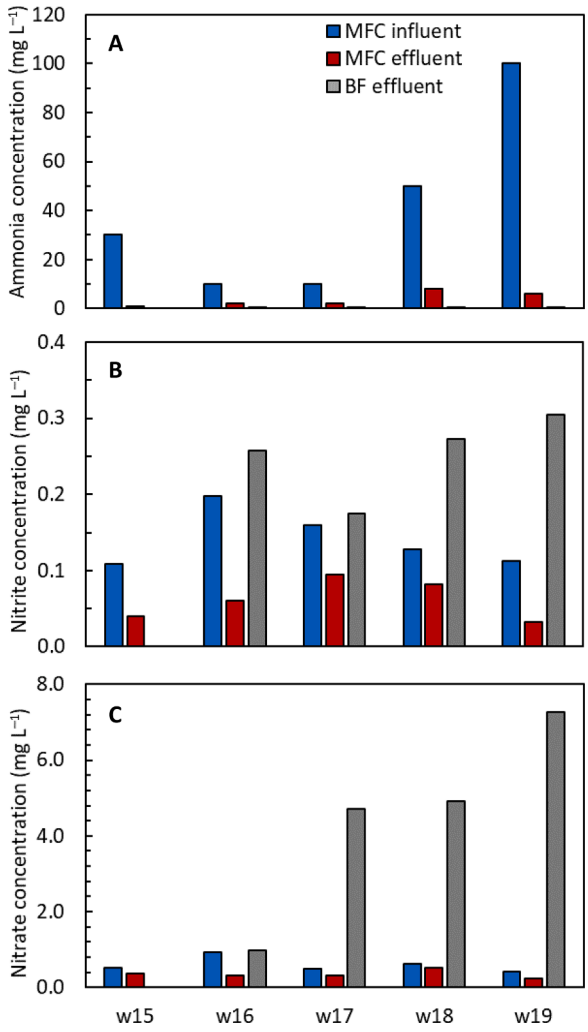


**Fig. 7.** Concentration of (A) ammonia, (B) nitrite and (C) nitrate in the MFC influent, effluent and post BF treatment.

concentration followed a trend similar to the nitrite, with a 41% decrease in the MFC (from 0.78 ± 0.40 mg $L^{-1}$ to 0.47 ± 0.31 mg $L^{-1}$), followed by an increase in the BF effluent in the latter weeks of operation (3.1 ± 2.7 mg $L^{-1}$ from week 13 to week 19). The total nitrogen concentration, decreased during the MFC/BF treatment, from 64 ± 1 mg $L^{-1}$ in the MFC influent, to 29 ± 3 mg $L^{-1}$ in the MFC effluent and 11 ± 4 mg $L^{-1}$ post BF treatment, indicating that the higher nitrate and nitrite concentrations in the BF effluent were due to nitrification. The average sulfide and phosphorus concentrations are reported in the Supporting Information.

The quality of the wastewater in the MFC influent, MFC effluent and BF effluent was analyzed in terms of $BOD_5$, fecal coliforms and *E. coli* concentrations in a one-month period collecting two samples per week (Supporting Information). The $BOD_5$ concentration followed a similar trend to that of the COD with a decrease of 70% in the MFC and of 91% post BF treatment. The average influent $BOD_5$ was 146 mg $L^{-1}$, which decreased to 44 mg $L^{-1}$ in the MFC effluent and 13 mg $L^{-1}$ in the BF effluent. The fecal coliforms and *E. coli* concentration decreased by two orders of magnitude through the MFC (fecal coliforms, influent = 91,000 MPN $mL^{-1}$; effluent = 810 MPN $mL^{-1}$; *E. coli*, influent = 72,000 MPN $mL^{-1}$; effluent = 790 MPN $mL^{-1}$). In the first two weeks of operation, the fecal coliforms and *E. coli* concentration in the BF effluent was 610 MPN $mL^{-1}$ for both the strains. The concentration of fecal coliforms and *E. coli* was only 0.075 MPN $mL^{-1}$ in the first three samples and increased to 24 MPN $mL^{-1}$ in the last sample. It was not clear if the higher content of microorganisms in the latter sample was due to a contamination during sampling or a decrease in the disinfection capability of the BF unit. To investigate the impact of the ultrafiltration system on the BF disinfection capacity, the UF membrane was removed over the last two weeks of operation and the concentration of fecal coliforms and *E. coli* in the BF effluent was compared with that obtained in the presence of the UF unit. The concentration of the fecal coliforms and *E. coli* increased by two orders of magnitude in the absence of the UF unit (fecal coliforms = 220 MPN $mL^{-1}$; *E. coli* = 180 MPN $mL^{-1}$ over the last two weeks of operation), suggesting that the ultrafiltration was more effective than the UV in reducing the content of microorganisms in the BF effluent.

At the end of the demonstration stage, approximately after six months from the time of inoculation, the mass of sludge accumulated in the MFC over the whole demonstration period was measured and analyzed in terms of TSS and VSS content. The total wet weight of sludge was 88.2 kg, with a TSS of 40 ± 3 g $L^{-1}$ and a VSS of 23 ± 2 g $L^{-1}$. The volume of wet sludge was approximately 91 L, corresponding to a sludge accumulation of 0.9 L per 1000 L of wastewater treated and a sludge production of 0.16 kg TSS per kg of COD removed. Conventional aerobic processes typically generate 0.32 kg TSS per kg COD removed (Ginestet and Camacho, 2007), therefore, 50% less sludge was generated in the MFC compared to conventional treatment.

### 3.4. Implications in the development and integration of MFCs in the wastewater treatment infrastructure

We developed, deployed, and evaluated over six months the performance of the largest air-cathode MFC ever produced, providing data that can help with our insight for achieving practical deployment of bioelectrochemical systems in wastewater treatment plants. The reactor startup was relatively fast even under challenging conditions of wastewater availability due to the low flow into the wet well, suggesting that these systems could be used for rapid deployment. Less than 5% of the energy consumed by the pump to deliver the wastewater from the wet well to the MFC was recovered as electrical energy. For example, after three months of operation, the MFC produced 11.4 Wh at 1.89 Lpm (average power of 1.29 ± 0.04 W over 9 h), corresponding to only 3% of the energy consumed by the pump (401 Wh). However, the energy generation in the MFC can likely be increased by maintaining a stable flow rate of a high strength wastewater. Even though the energy recovery and the power generation by the MFC were lower than expected, the combined MFC/BF technology treated domestic wastewater with a minimal energy consumption of only 0.13 Wh/L, which is more than 75% lower than that of conventional wastewater treatment (0.6 Wh/L) (McCarty et al., 2011). Throughout the demonstration, the MFC treated approximately 110 $m^3$ of wastewater producing an average of 18 Wh $m^{-3}$ (88 Wh $kg_{COD}^{-1}$) of wastewater treated with peaks of 37 Wh $m^{-3}$ over a week of operation.

The MFC/BF effluent quality met the water quality requirements for discharge from non-municipal sewage treatment facilities for most of the parameters investigated. Ammonia (4 mg $L^{-1}$), nitrate (10 mg $L^{-1}$), pH (9.0), TSS (30 mg $L^{-1}$) and organic content (25 mg $L^{-1}$) were all lower than the average monthly limit for discharge. Fecal coliforms were reduced below the required limit (20 MPN $mL^{-1}$) only in the first three weeks of operation and were approximately nine times larger than the maximum limit in the last five samples, indicating that higher stability of treatment performance should be achieved to avoid additional steps in the effluent disposal and the associated costs. Phosphorus concentration in the BF effluent was approximately 15 times larger than the maximum average monthly limit (4 mg $L^{-1}$), requiring further approaches to manage the concentration of this chemical.

Maintaining power density during system scale up is challenging, but as shown here the volume of the reactor can be increased while producing power densities only slightly less than those obtained using smaller systems. The pilot-scale MFC maximum power density was 0.072 W $m^{-2}$ based on the overall cathode area (20 $m^2$) and 0.092 W $m^{-2}$ neglecting the

area of the cathode occupied by the stainless steel frame, which decreased the electroactive area by 22%. This power density is around one third of that previously reported for a 0.028 L cubic MFC (0.31 ± 0.01 W $m^{-2}$) fed domestic wastewater using the same anode and cathode materials and electrode spacing, even though the active volume in the pilot MFC was 30,000 times larger. This indicated that the electrode power density could be maintained in pilot-scale MFCs if the reactor size was scaled up using reactor configurations similar to lab-scale MFCs.

The power densities of the large air-cathode MFC examined here were substantially higher than previous bioelectrochemical systems of similar scales (≥250 L). The maximum power density in a previous study for a 250 L air-cathode MFC was 0.057 ± 1 W $m^{-2}$, about 21% lower than that reported here (0.072 W $m^{-2}$), and used a precious metal catalyst (Pt) on the cathodes compared to activated carbon used here (Feng et al., 2014). The maximum volumetric power density was 0.46 W $m^{-3}$, which is less than one-third of that obtained here (1.68 W $m^{-3}$) (Feng et al., 2014). The low volumetric power density was a consequence of the low electrode packing density in that study (8 $m^2$ $m^{-3}$) compared to 23 $m^2$ $m^{-3}$ here. A maximum power density of only 0.007 W $m^{-2}$ was reported in another study using a 720 L (6 reactors each of 120 L) air-cathode MFC (Das et al., 2020), which is one order of magnitude smaller than that obtained here. The much lower power density was likely a combination of the use of flat anodes (carbon felt), which produce lower power than carbon brushes (Yang et al., 2017), and the low electrode packing density of the reactor (1.3 $m^2$ $m^{-3}$).

The air-cathode MFC examined here also had improved performance compared to large MFCs using aerated catholytes. For example, tests using a 1500 L MFC achieved maximum power densities of 0.036 W $m^{-2}$ (Dong et al., 2019) in one study, and 0.029 W $m^{-2}$ (0.40 W $m^{-3}$) in other tests (He et al., 2019). Using aerated catholytes decreases the energy efficiency of the MFCs due to the need to sparge air in the catholyte. High power densities have been reported for other MFCs which were defined as large scale systems based on total system volume, but were constructed by combining several small scale systems, so the power densities were not obtained for larger reactors (Babanova et al., 2020; Blatter et al., 2021; Ge and He, 2016; Liang et al., 2019). For example, a total system volume of 200 L was obtained by connecting 96 MFCs of two liters each (Ge and He, 2016), and a 1000 L reactor was fabricated by using 50 modules that were 20 L each (Liang et al., 2019), potentially increasing the capital cost of the MFC and the complexity of the power conditioning board.

Minimizing the MFC internal resistance has been shown to be the most effective strategy to increase the performance of lab-scale MFCs. Due to the low conductivity of the wastewater, reducing the electrode spacing has been shown to decrease the internal resistance of MFCs and increase the reactor performance (Logan et al., 2018). Unfortunately, reducing the electrode spacing could lead to short-circuiting the cell if the electrodes were to touch each other, requiring the installation of separators between the electrodes to ensure better electrical insulation, further increasing the cost of the materials. The MFC internal resistance can be further reduced by diminishing the anode and cathode resistances, primarily by reducing the development of pH differences between the electrodes. Forcing the flow through closely spaced electrodes has recently been shown to greatly improve power generation (Rossi and Logan, 2021; Rossi et al., 2021), although additional considerations must be included to remove particles entering the MFC to minimize clogging. Based on the results of this study, further improvements of MFC technology are needed prior to its transition into use in wastewater treatment facilities. Future research should focus on improving the throughput and energy production of the technology, with the goal of reducing capital costs and reactor footprint by increasing electrode packing densities.

## 4. Conclusions

The performance of the largest air-cathode MFC developed to date was investigated over a six-month period using domestic and industrial wastewater. The air cathodes avoided the need for aeration of the wastewater that was serially pumped through 17 anode modules (11 $m^2$) connected to 32 cathodes (20 $m^2$). The MFC started producing useful electricity only three days after startup, showing a large impact of the availability of wastewater on current and power generation. The average power produced over six months was 0.46 ± 0.35 W at an average current of 1.54 ± 0.90 A with a peak of 1.43 W and 2.95 A recorded 81 days after inoculation. The anode-cathode pairs produced variable current and power depending on the wastewater flow rate and their position in the MFC, with the modules in the middle of the reactor producing nearly 4 times more current due to the higher available cathode area and lower oxygen intrusion in the media. The MFC removed 49 ± 15 % of the COD with a Coulombic efficiency of approximately 9% while up to 91 ± 6 % of the COD was removed in the combined MFC/BF process. $BOD_5$, ammonia, nitrate, nitrite, TSS, *E. coli* and fecal coliforms were drastically abated in the MFC, with removal up to 90% for chemicals ($BOD_5$, ammonia) and 99% for bacteria in the MFC/BF overall technology. The combined MFC/BF treated domestic wastewater with a minimal energy consumption of only 0.13 Wh/L, which is more than 50% lower than that of conventional wastewater treatment. The pilot study presented here provides a path forward for the MFC technology, showing that MFCs can be effectively integrated into the existing wastewater treatment infrastructure, producing electricity while efficiently treating wastewater.

## Declaration of Competing Interest

The authors declare that they have no known competing financial interests or personal relationships that could have appeared to influence the work reported in this paper.

## Acknowledgments

The authors acknowledge funding by the Environmental Security Technology Certification Program via cooperative research agreement W9132T-16-2-0014 through the US Army Engineer Research and Development Center. The authors acknowledge CDM Smith and Intuitech for their contributions in the design and manufacturing of the MFC.

## Supplementary materials

Supplementary material associated with this article can be found, in the online version, at doi:10.1016/j.watres.2022.118208.

## References

An, J., Li, N., Wan, L., Zhou, L., Du, Q., Li, T., Wang, X., 2017. Electric field induced salt precipitation into activated carbon air-cathode causes power decay in microbial fuel cells. Water Res. 123, 369–377. https://doi.org/10.1016/j.watres.2017.06.087.

Babanova, S., Jones, J., Phadke, S., Lu, M., Angulo, C., Garcia, J., Carpenter, K., Cortese, R., Chen, S., Phan, T., Bretschger, O., 2020. Continuous flow, large-scale, microbial fuel cell system for the sustained treatment of swine waste. Water Environ. Res. 92, 60–72. https://doi.org/10.1002/wer.1183.

Blatter, M., Delabays, L., Furrer, C., Huguenin, G., Cachelin, C.P., Fischer, F., 2021. Stretched 1000-L microbial fuel cell. J. Power Sources 483. https://doi.org/10.1016/j.jpowsour.2020.229130.

Bouwman, L., Van Houtven, D., Pant, D., Gallego, Y.A., Vanbroekhoven, K., 2020. Carbon based electrode with large geometric dimensions. US 2020/0295381 A1.

Cheng, S., Logan, B.E., 2011. Increasing power generation for scaling up single-chamber air cathode microbial fuel cells. Bioresour. Technol. 102, 4468–4473. https://doi.org/10.1016/j.biortech.2010.12.104.

Daims, H., Wagner, M., Seviour, R.J., 2010. Microbial ecology of activated sludge. London, UK.

Das, I., Ghangrekar, M.M., Satyakam, R., Srivastava, P., Khan, S., Pandey, H.N., 2020. On-site sanitary wastewater treatment system using 720-L stacked microbial fuel cell: case study. J. Hazardous, Toxic, Radioact. Waste 24, 04020025. https://doi.org/10.1061/(asce)hz.2153-5515.0000518.

Dekker, A., Ter Heijne, A., Saakes, M., Hamelers, H.V.M., Buisman, C.J.N., 2009. Analysis and improvement of a scaled-up and stacked microbial fuel cell. Environ. Sci. Technol. 43, 9038–9042. https://doi.org/10.1021/es901939r.

Do, M.H., Ngo, H.H., Guo, W.S., Liu, Y., Chang, S.W., Nguyen, D.D., Nghiem, L.D., Ni, B. J., 2018. Challenges in the application of microbial fuel cells to wastewater

treatment and energy production: A mini review. Sci. Total Environ. 639, 910–920. https://doi.org/10.1016/j.scitotenv.2018.05.136.
Dong, Y., He, W., Liang, D., Li, C., Liu, G., Liu, J., Ren, N., Feng, Y., 2019. Operation strategy of cubic-meter scale microbial electrochemistry system in a municipal wastewater treatment plant. J. Power Sources 441, 227124. https://doi.org/10.1016/j.jpowsour.2019.227124.
Feng, Y., He, W., Liu, J., Wang, X., Qu, Y., Ren, N., 2014. A horizontal plug flow and stackable pilot microbial fuel cell for municipal wastewater treatment. Bioresour. Technol. 156, 132–138. https://doi.org/10.1016/j.biortech.2013.12.104.
Ge, Z., He, Z., 2016. Long-term performance of a 200 liter modularized microbial fuel cell system treating municipal wastewater: Treatment, energy, and cost. Environ. Sci. Water Res. Technol. 2, 274–281. https://doi.org/10.1039/c6ew00020g.
Ginestet, P., Camacho, P., 2007. Technical evaluation of sludge production and reduction. Comparative evaluation of sludge reduction routes, 5. IWA Publishing. https://doi.org/10.2166/9781780402352. ISBN electronic: 9781780402352. Publication date: October 2006.
He, W., Dong, Y., Li, C., Han, X., Liu, G., Liu, J., Feng, Y., 2019. Field tests of cubic-meter scale microbial electrochemical system in a municipal wastewater treatment plant. Water Res. 155, 372–380. https://doi.org/10.1016/j.watres.2019.01.062.
He, W., Wallack, M.J., Kim, K.Y., Zhang, X., Yang, W., Zhu, X., Feng, Y., Logan, B.E., 2016. The effect of flow modes and electrode combinations on the performance of a multiple module microbial fuel cell installed at wastewater treatment plant. Water Res. 105, 351–360. https://doi.org/10.1016/j.watres.2016.09.008.
Heidrich, E.S., Curtis, T.P., Dolfing, J., 2011. Determination of the internal chemical energy of wastewater. Environ. Sci. Technol. 45, 827–832. https://doi.org/10.1021/es103058w.
Hiegemann, H., Littfinski, T., Krimmler, S., Lübken, M., Klein, D., Schmelz, K.G., Ooms, K., Pant, D., Wichern, M., 2019. Performance and inorganic fouling of a submergible 255 L prototype microbial fuel cell module during continuous long-term operation with real municipal wastewater under practical conditions. Bioresour. Technol. 294 https://doi.org/10.1016/j.biortech.2019.122227.
Holmes, D.E., Bond, D.R., O'Neil, R.A., Reimers, C.E., Tender, L.R., Lovley, D.R., 2004. Microbial communities associated with electrodes harvesting electricity from a variety of aquatic sediments. Microb. Ecol. 48, 178–190. https://doi.org/10.1007/s00248-003-0004-4.
Huang, L., Chai, X., Quan, X., Logan, B.E., Chen, G., 2012. Reductive dechlorination and mineralization of pentachlorophenol in biocathode microbial fuel cells. Bioresour. Technol. 111, 167–174. https://doi.org/10.1016/j.biortech.2012.01.171.
Jung, R.K., Zuo, Y., Regan, J.M., Logan, B.E., 2008. Analysis of ammonia loss mechanisms in microbial fuel cells treating animal wastewater. Biotechnol. Bioeng. 99, 1120–1127. https://doi.org/10.1002/bit.21687.
Kim, J.R., Beecroft, N.J., Varcoe, J.R., Dinsdale, R.M., Guwy, A.J., Slade, R.C.T., Thumser, A., Avignone-Rossa, C., Premier, G.C., 2011. Spatiotemporal development of the bacterial community in a tubular longitudinal microbial fuel cell. Appl. Microbiol. Biotechnol. 90, 1179–1191. https://doi.org/10.1007/s00253-011-3181-y.
Kim, K.Y., Yang, W., Logan, B.E., 2015. Impact of electrode configurations on retention time and domestic wastewater treatment efficiency using microbial fuel cells. Water Res. 80, 41–46. https://doi.org/10.1016/j.watres.2015.05.021.
Li, Z.L., Zhu, Z.L., Lin, X.Q., Chen, F., Li, X., Liang, B., Huang, C., Zhang, Y.M., Sun, K., Zhou, A.N., Wang, A.J., 2021. Microbial fuel cell-upflow biofilter coupling system for deep denitrification and power recovery: Efficiencies, bacterial succession and interactions. Environ. Res. 196 https://doi.org/10.1016/j.envres.2020.110331.
Liang, D., He, W., Li, C., Wang, F., Crittenden, J.C., Feng, Y., 2021. Remediation of nitrate contamination by membrane hydrogenotrophic denitrifying biofilm integrated in microbial electrolysis cell. Water Res. 188, 116498 https://doi.org/10.1016/j.watres.2020.116498.
Liang, F., Xiao, Y., Zhao, F., 2013. Effect of pH on sulfate removal from wastewater using a bioelectrochemical system. Chem. Eng. J. 218, 147–153. https://doi.org/10.1016/j.cej.2012.12.021.
Liang, P., Duan, R., Jiang, Y., Zhang, X., Qiu, Y., Huang, X., 2019. Corrigendum to "One-year operation of 1000-L modularized microbial fuel cell for municipal wastewater treatment. Water Res. 166, 114878 https://doi.org/10.1016/j.watres.2019.114878.
Liang, P., Duan, R., Jiang, Y., Zhang, X., Qiu, Y., Huang, X., 2018. One-year operation of 1000-L modularized microbial fuel cell for municipal wastewater treatment. Water Res. 141, 1–8. https://doi.org/10.1016/J.WATRES.2018.04.066.
Lin, W.C., Lin, W.C., Coppi, M.V, Coppi, M.V, Lovley, D.R., Lovley, D.R., 2004. Geobacter sulfurreducens can grow with oxygen as a terminal electron acceptor. Appl. Environ. Microbiol. 70, 2525–2528. https://doi.org/10.1128/AEM.70.4.2525.
Liu, F., Sun, L., Wan, J., Tang, A., Deng, M., Wu, R., 2019. Organic matter and ammonia removal by a novel integrated process of constructed wetland and microbial fuel cells. RSC Adv. 9, 5384–5393. https://doi.org/10.1039/c8ra10625h.
Logan, B.E., Rossi, R., Ragab, A., Saikaly, P.E., 2019. Electroactive microorganisms in bioelectrochemical systems. Nat. Rev. Microbiol. 17 https://doi.org/10.1038/s41579-019-0173-x.
Logan, B.E., Wallack, M.J., Kim, K.Y., He, W., Feng, Y., Saikaly, P.E., 2015. Assessment of microbial fuel cell configurations and power densities. Environ. Sci. Technol. Lett. 2, 206–214. https://doi.org/10.1021/acs.estlett.5b00180.
Logan, B.E., Zikmund, E., Yang, W., Rossi, R., Kim, K.-Y., Saikaly, P.E., Zhang, F., 2018. Impact of ohmic resistance on measured electrode potentials and maximum power production in microbial fuel cells. Environ. Sci. Technol. 52, 8977–8985. https://doi.org/10.1021/acs.est.8b02055.
Lu, L., Guest, J.S., Peters, C.A., Zhu, X., Rau, G.H., Ren, Z.J., 2018. Wastewater treatment for carbon capture and utilization. Nat. Sustain. 1, 750–758. https://doi.org/10.1038/s41893-018-0187-9.
McCarty, P.L., Bae, J., Kim, J., 2011. Domestic wastewater treatment as a net energy producer - can this be achieved? Environ. Sci. Technol. 45, 7100–7106. https://doi.org/10.1021/es2014264.
Motoyama, A., Ichihashi, O., Hirooka, K., 2021. Is ammonia volatilization a main mechanism of ammonia loss in single-chamber microbial fuel cells? Int. J. Environ. Sci. Technol. 18, 781–786. https://doi.org/10.1007/s13762-020-02895-7.
Munoz-Cupa, C., Hu, Y., Xu, C., Bassi, A., 2021. An overview of microbial fuel cell usage in wastewater treatment, resource recovery and energy production. Sci. Total Environ. 754, 142429 https://doi.org/10.1016/j.scitotenv.2020.142429.
Popat, S.C., Torres, C.I., 2016. Critical transport rates that limit the performance of microbial electrochemistry technologies. Bioresour. Technol. 215, 265–273. https://doi.org/10.1016/j.biortech.2016.04.136.
Rossi, R., Baek, G., Saikaly, P.E., Logan, B.E., 2021. Continuous flow microbial flow cell with an anion exchange membrane for treating low conductivity and poorly buffered wastewater. ACS Sustain. Chem. Eng. 9, 2946–2954. https://doi.org/10.1021/acssuschemeng.0c09144.
Rossi, R., Cario, B.P., Santoro, C., Yang, W., Saikaly, P.E., Logan, B.E., 2019. Evaluation of electrode and solution area-based resistances enables quantitative comparisons of factors impacting microbial fuel cell performance. Environ. Sci. Technol. 53 https://doi.org/10.1021/acs.est.8b06004.
Rossi, R., Evans, P.J., Logan, B.E., 2019a. Impact of flow recirculation and anode dimensions on performance of a large scale microbial fuel cell. J. Power Sources 412, 294–300. https://doi.org/10.1016/j.jpowsour.2018.11.054.
Rossi, R., Hall, D.M., Wang, X., Regan, J.M., Logan, B.E., 2020. Quantifying the factors limiting performance and rates in microbial fuel cells using the electrode potential slope analysis combined with electrical impedance spectroscopy. Electrochim. Acta 348, 136330. https://doi.org/10.1016/j.electacta.2020.136330.
Rossi, R., Jones, D., Myung, J., Zikmund, E., Yang, W., Alvarez, Y., Pant, D., Evans, P.J., Page, M.A., Cropek, D.M., Logan, B.E., 2019b. Evaluating a multi-panel air cathode through electrochemical and biotic tests. Water Res. 148, 51–59. https://doi.org/10.1016/j.watres.2018.10.022.
Rossi, R., Logan, B.E., 2021. Using an anion exchange membrane for effective hydroxide ion transport enables high power densities in microbial fuel cells. Chem. Eng. J. 422, 130150 https://doi.org/10.1016/j.cej.2021.130150.
Sayess, R.R., Saikaly, P.E., El-Fadel, M., Li, D., Semerjian, L., 2013. Reactor performance in terms of COD and nitrogen removal and bacterial community structure of a three-stage rotating bioelectrochemical contactor. Water Res. 47, 881–894. https://doi.org/10.1016/j.watres.2012.11.023.
Shehab, N., Li, D., Amy, G.L., Logan, B.E., Saikaly, P.E., 2013. Characterization of bacterial and archaeal communities in air-cathode microbial fuel cells, open circuit and sealed-off reactors. Appl. Microbiol. Biotechnol. 97, 9885–9895. https://doi.org/10.1007/s00253-013-5025-4.
Velasquez-Orta, S.B., Curtis, T.P., Logan, B.E., 2009. Energy from algae using microbial fuel cells. Biotechnol. Bioeng. 103, 1068–1076. https://doi.org/10.1002/bit.22346.
Vilajeliu-Pons, A., Puig, S., Salcedo-Dávila, I., Balaguer, M.D., Colprim, J., 2017. Long-term assessment of six-stacked scaled-up MFCs treating swine manure with different electrode materials. Environ. Sci. Water Res. Technol. 3, 947–959. https://doi.org/10.1039/c7ew00079k.
Wang, J., Song, X., Li, Q., Bai, H., Zhu, C., Weng, B., Yan, D., Bai, J., 2019. Bioenergy generation and degradation pathway of phenanthrene and anthracene in a constructed wetland-microbial fuel cell with an anode amended with nZVI. Water Res. 150, 340–348. https://doi.org/10.1016/j.watres.2018.11.075.
Ward, L., Page, M., Jurevis, J., Nelson, A., Rivera, M., Hernandez, M., Chappell, M., Dusenbury, J., 2015. Assessment of biologically active GAC and complementary technologies for gray water treatment. J. Water Reuse Desalin. 5, 239–249. https://doi.org/10.2166/wrd.2015.088.
Yang, N., Zhan, G., Li, D., Wang, X., He, X., Liu, H., 2019. Complete nitrogen removal and electricity production in Thauera-dominated air-cathode single chambered microbial fuel cell. Chem. Eng. J. 356, 506–515. https://doi.org/10.1016/j.cej.2018.08.161.
Yang, N., Zhan, G., Wu, T., Zhang, Y., Jiang, Q., Li, D., Xiang, Y., 2018. Effect of air-exposed biocathode on the performance of a Thauera-dominated membraneless single-chamber microbial fuel cell (SCMFC). J. Environ. Sci. 66, 216–224. https://doi.org/10.1016/j.jes.2017.05.013.
Yang, Q., Liang, S., Liu, J., Lv, J., Feng, Y., 2017. Analysis of anodes of microbial fuel cells when carbon brushes are preheated at different temperatures. Catalysts 7, 312–320. https://doi.org/10.3390/catal7110312.
Yuan, J., Yuan, H., Huang, S., Liu, L., Fu, F., Zhang, Y., Cheng, F., Li, J., 2021. Comprehensive performance, bacterial community structure of single-chamber microbial fuel cell affected by COD/N ratio and physiological stratifications in cathode biofilm. Bioresour. Technol. 320, 124416 https://doi.org/10.1016/j.biortech.2020.124416.
Zhang, F., Ge, Z., Grimaud, J., Hurst, J., He, Z., 2013. Long-term performance of liter-scale microbial fuel cells treating primary effluent installed in a municipal wastewater treatment facility. Environ. Sci. Technol. 47, 4941–4948. https://doi.org/10.1021/es400631r.
Zhang, G., Jiao, Y., Lee, D.J., 2015. A lab-scale anoxic/oxic-bioelectrochemical reactor for leachate treatments. Bioresour. Technol. 186, 97–105. https://doi.org/10.1016/j.biortech.2015.03.022.
Zheng, D., Gu, W., Zhou, Q., Zhang, L., Wei, C., Yang, Q., Li, D., 2020. Ammonia oxidation and denitrification in a bio-anode single-chambered microbial electrolysis cell. Bioresour. Technol. 310, 123466 https://doi.org/10.1016/j.biortech.2020.123466.